Int. J. Adv. Res. Sci. Technol. Volume 3, Issue1, 2014, pp.44-50 # ICV 5.14

IJARST

International Journal of Advanced Research in Science and Technology

journal homepage: www.ijarst.com

ISSN 2319 – 1783 (Print)

ISSN 2320 – 1126 (Online)

Photoelectrochemical studies of nonstoichiometric nanostructured PbO_x using $Fe(CN)_6^{-4/-3}$ as an active electrolyte in ionic liquid

Dipal B Patel and Indrajit Mukhopadhyay*

School of Solar Energy, Pandit Deendayal Petroleum University, Raisan, Gandhinagar-382007, India.

****Corresponding Author's Email: indrajit.m@sse.pdpu.ac.in, Fax: +91-79-23275030; Tel: +91-79- 23275303;***

ARTICLEINFO

Article history:

Received 05 May 2014

Accepted 19 May 2014

Available online 24 May 2014

Keywords:

Photoelectrochemical cell,
Nonstoichiometric,
Nanostructured
Ionic liquid,
α -PbO and β -PbO

ABSTRACT

Photoactive nanostructured lead oxide was prepared by applying DC potential pulse in alkaline sodium sulfate solution at 80^0C. The resulting oxide thin film showed vertically aligned interconnected nanowall assemblies all over the active substrate. The film was characterized by XRD, SEM, EDX and UV-vis diffuse reflectance spectroscopy. The UV-vis measurements confirmed an optical band gap of 1.95 and 2.71 eV, which can be attributed to the phases respectively α-PbO and β-PbO. Photoelectro chemical measurements under chopped white light illumination condition in ionic liquid (BMIm Cl^-) medium showed a stable photoresponse extending to a wider potential range of 3.7 V compared to only 1.7 V in aqueous medium. Typical photocurrent densities of 3.01 and 4.03 mA/cm^2 were obtained from ionic liquid and aqueous medium, respectively. The JV characteristic of a PEC cell indicates a low V_{oc} of 273 mV in ionic liquid medium compared to 768 mV in aqueous medium. The low V_{oc} is attributed to the shift of the redox potential of the active electrolyte in ionic liquid.

© 2014 International Journal of Advanced Research in Science and Technology (IJARST). All rights reserved.

Introduction:

Historically acidic medium is being used to study the photoeffects of the anodized lead electrodes by many groups [1–10]. Although both the α-PbO and β-PbO are photoactive phases of anodized lead, the contribution from α-PbO in photoresponse is major. The corrosion of PbO electrodes due to acidic environment was the main drawback of the PEC cell constructed from acidic medium as an active electrolyte. To overcome this problem, alkaline sodium sulfate solutions have been adopted by many researchers [7, 11–13]. Different electrochemical anodization techniques have been tried to make photoactive phases of PbO out of lead metal [14–17]. Among all the techniques, potentiodynamic anodization is mostly used and hence understood thoroughly [12, 16–18]. Many groups have explored different approaches for anodization, like pulse coupled potentiodynamic [14], potentiostatic [15] and modified window potentiodynamic [16, 17]. Effect of bath temperature and anodization time is also studied by few groups [12,19] . The α-PbO has got more attraction and studied well because of its major contribution to photoactivity compared to β-PbO [20]. Many groups have concluded that (110) plane of the α-PbO leads to a better photoactive film [15]. In spite of many efforts, the photocurrent more than 4-5 mA/cm^2 and an open circuit photopotential of 800 mV is still a challenging task. The photoelectrochemical properties of anodized PbO in both acidic and alkaline mediums have been studied by several researchers. Most of these studies were done in aqueous electrolytes.

In this manuscript, we present an efficient electrochemical route for the synthesis of vertically aligned interconnected nanowalls of PbO_x by potential pulse technique in hot aqueous alkaline medium. We have studied the photoresponse of the oxide thin film in 1-butyl-3-methylimidazolium chloride (BMIm Cl^-) ionic liquid medium using $Fe(CN)_6^{-4/-3}$ as an active electrolyte. The influence of ionic liquid medium on the photoelectrochemical properties of anodized film is compared with an aqueous medium.

Experimental:

The electrochemical cell used for this study is a well-known three electrode arrangement with working, counter and reference electrodes. The chemicals NaOH, Na_2SO_4 , $K_4Fe(CN)_6$ and $K_3Fe(CN)_6$ as received, and double distilled water (Milli-Q) were used to carry out

all the experiments. A lead metal having an effective geometric area 0.25 cm^2 cut from a lead foil (99.999% pure, Alfa Aesar) was used as a working electrode (WE). The Pb electrodes were soldered from backside with Teflon coated copper wire and insulated with acrylic paste, leaving only the front surface free for the anodization. A platinum foil of area 2 cm^2 and Hg/HgO electrodes were used as a counter (CE) and reference electrode (RE), respectively. Prior to anodization, the lead electrode surface was polished with paper of grit designation P800 (surface of particle size 21.8 µm) and washed with double distilled water. A 0.1 M NaOH (Prepared in 0.1 M Na_2SO_4) solution was used as an active electrolyte for the anodization. Electrochemical polishing of lead electrode was done just before anodization to remove organic and inorganic impurities from the surface. Potential pulse anodization was carried out by a potentiostat/galvanostat (PGSTAT302N, Autolab) with the potential pulse between 0.6 to 0.1 V with 50% duty cycle at 80 °C. This potential pulse was selected after number of experiments for optimizing the step from a wide potential window. After anodization, the electrodes were washed thoroughly with double distilled water and sintered at 130 °C for 30 min in hot air oven.

Structural, morphological and optical characterizations of the oxide film obtained under optimum conditions were carried out by X-ray diffraction (X'Pert PRO, PANalytical), Scanning electron microscope (Ultra-55, Zeiss) equipped with EDX (Oxford) and UV-visible diffuse reflectance spectroscopy (Shimadzu-2600), respectively. Both photocurrent and capacitance measurements were performed using a photoelectrochemical cell (PEC) with the configuration:

PbO_x (0.25 cm^2) film | 0.1 M $K_4Fe(CN)_6$ / 0.01 $K_3Fe(CN)_6$ (pH 9.2) | Pt (2 cm^2).

However, due to the lower solubility of $Fe(CN)_6^{-4/-3}$ in ionic liquid medium we have used saturated active electrolyte. The light source used for the PEC measurements was a 125 W / 12 V tungsten halogen lamp. High-density silicone photodetector was used for normalizing the lamp spectrum with that of solar spectrum. The IV measurements were performed using class AAA solar simulator (SS50AAA, Photo Emission Tech., Inc.). The stability of the anodized electrodes was studied under constant illumination conditions. The two electrode PEC cell assembly without any reference electrode was used to study the effect of constant illumination on the stability of the photoanode in both the electrolytes (viz. aqueous and ionic liquid). All the potentials for PEC studies are presented with respect to (a. Hg/HgO, 3 M KOH, +0.098 V vs. NHE) in the case of aqueous electrolyte and (b. Platinum quasi reversible electrode, +0.6 V vs. NHE) in the case of ionic liquid medium.

Results and Discussion:

Cyclic voltammetry:

A cyclic voltammogram of the Pb electrode in 0.1 M NaOH (prepared in 0.1 M Na_2SO_4) at 80 °C with a sweep rate of 200 mV/s is shown in Figure-1. In the positive sweep, two anodic peaks A_1 and A_2 were observed, indicating the step-wise oxidation of Pb to PbO and PbO to PbO_2, respectively. While in the negative sweep, single anodic peak, C_1 was observed, which can be attributed to the reduction of PbO_2 to PbO. The occurrence of a very small current at the extreme negative end (C_2) is due to a partial reduction of PbO [12].

Taking all these in to consideration, here in this study we have explored the possibilities of a potential pulse anodization of Pb metal. To start with the optimization the potential pulse anodization with different combinations of step potentials in the range of anodic peaks were applied for different time at 80 °C. The potential pulse position, pulse width, interval time and duty cycle, were optimized and it was found that the electrode anodized from a potential pulse between 0.6 to 0.1 V (pulse structure as shown in Figure-2) for 800 s gives the best photoresponse. Hence the subsequence studies were carried out for the best photo electrode.

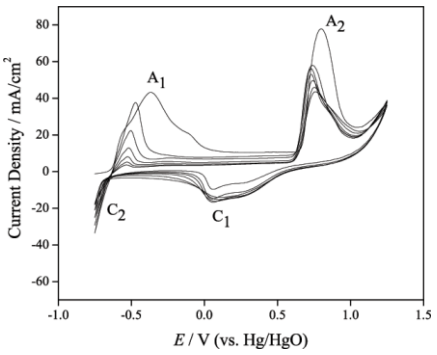

Fig: 1. A cyclic voltammogram (a few consecutive cycles) of lead in 0.1 M NaOH (prepared in 0.1 M Na_2SO_4) at 80^0C.

XRD analysis:

The phase identification of the oxide film obtained after the anodization was done by powder X-ray diffraction. Observed diffraction peaks from Figure-3 were identified as α-PbO [14,15,21,22] . The most intense line corresponds to the (110) plane of α-PbO with the d-spacing of 2.804 Å. The anodized film showed a preferential growth in (110) plane of α -PbO. As it can be seen from the XRD pattern that all the major peaks correspond to only α-PbO leaving no elemental Pb on the surface which further confirms highly crystalline and **uniform** anodized surface. The crystallite size (*D*) was derived from the FWHM of the XRD peak by using Scherrer formula [23],

$$D = \lambda/\beta \, Cos \, \theta \qquad (1)$$

Where β is the full width half maximum (FWHM), λ is the wavelength of the Cu-Kα X-rays (1.5406 Å). All the structural parameters extracted from the XRD spectra are listed in Table: 1. Overall, very high intensity of the diffraction lines indicates highly crystalline nature of the resulting oxide film.

UV-visible spectroscopy:

The diffuse reflectance spectroscopy (DRS) was employed on the anodized film using Shimadzu-2600 spectrophotometer equipped with integrated sphere. The sharp absorbance at two different energy levels (at 1.95 eV and 2.71 eV) indicate the presence of tetragonal (α) and orthorhombic (β) phases in the anodized film, as shown in Figure-4. It is interesting to note that the β-PbO phase absorbs strongly than the α-PbO. Although XRD pattern does not show any characteristic peak of β-PbO except the peak at 2θ = 54.79°, which is attributed to both α-PbO and β-PbO. This anomaly can be explained on the bases of either low crystallinity of β-PbO phase or its minimum content in resulting film. Hence, the UV study indicates that the anodized film contains photo active α-PbO phase with β-PbO as an impurity.

The bandgap values obtained from the Tauc plots (Figure-5) for direct (2.15 eV and 2.71 eV) and (insect of Figure-5) indirect bandgap (1.93 eV) calculations are in well agreement with those found from the UV-vis diffuse reflectance spectroscopy (2.71 eV and 1.95 eV).

Table: 1 The structural parameters extracted from the analysis of (110) peak of the XRD data

Parameter (unit)	Potential pulse technique	Standard technique[12]
d-spacing (Å)	2.804	2.803
Crystallite size (Å)	500	450
Micro strain (%)	0.2803	0.3113
FWHM (2θ)	0.1968	0.2135
Dislocation density (cm^{-2})	1.27×10^{15}	2.30×10^{15}
Lattice parameter (Å)	a=3.97& c=5.03	a=3.96& c=5.03

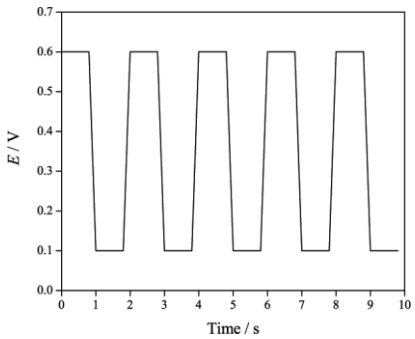

Fig: 2. A potential pulse structure used for the anodization of lead electrode.

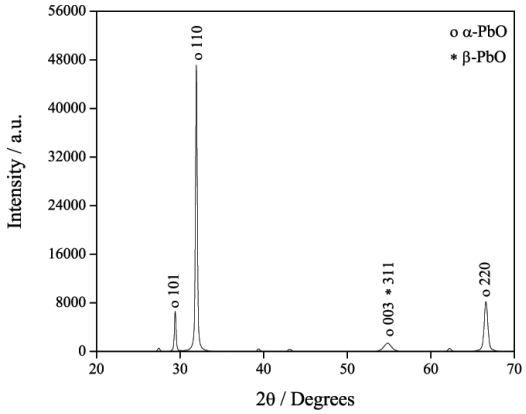

Fig: 3. The XRD pattern of the oxide film synthesized by potential pulse anodization followed by sintering for 30 min at 130 °C.

Surface morphological aspects:

The surface morphology of the anodized film was analyzed by scanning electron microscope (SEM). Application of potential pulse lead to an observable change in the morphology of the resulting oxide film, as shown in Figure-6. The surface morphology of the oxide film obtained by the potential pulse anodization shows vertically aligned interconnected oxide nano walls distributed uniformly all over the active area of the substrate. The presence of interconnected nano walls lead to an increase in the active surface area of the oxide film. The higher resolution image (Figure-6b) indicates a typical wall thickness of 60-80 nm. Comparison of Figure-6b and 6d clearly indicates that in the absence of any potential pulse the formation of oxide film takes place by the collision of irregular clusters in non-uniform manner. As seen from Figure-6b, the inter wall pore structure can have profound effect on the photoelectrochemistry. The EDX analysis confirms that the film is composed of elemental Pb and O and the oxide is nonstoichiometric in nature.

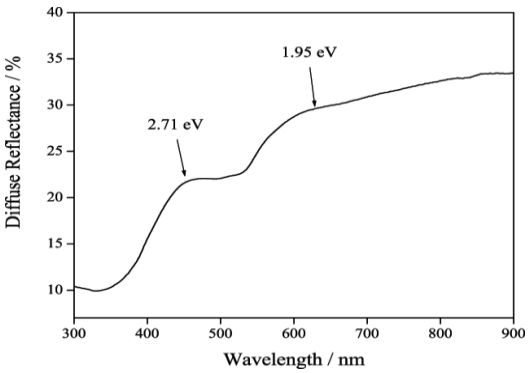

Fig: 4. Diffuse reflectance spectra of the oxide film synthesized by potential pulse anodization followed by sintering for 30 min at 130^0C

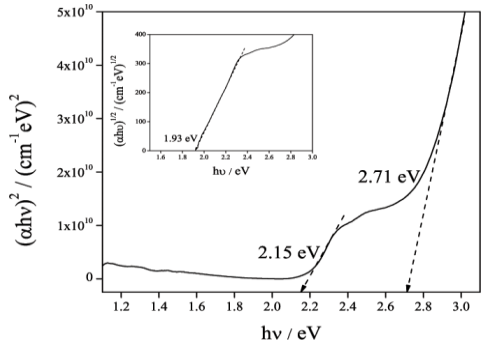

Fig: 5. Tauc plot for the determination of direct and indirect (insect) Bandgap of anodized PbO_x film

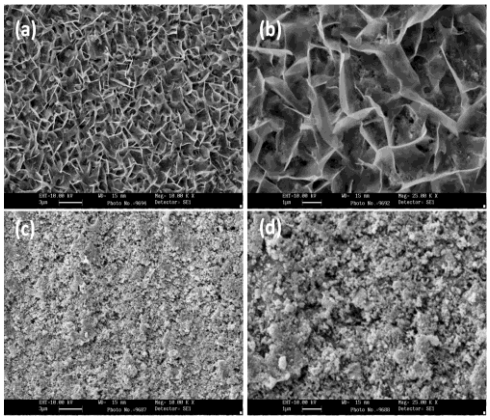

Fig: 6. SEM images showing the surface morphology of the lead oxide films anodized by potential pulse (a,b) and standard (c,d) method [12] at magnifications of X 5000 (a,c) and X 25000 (b,d).

Proposed growth mechanism:

The formation of the nano walls by the application of potential pulse clearly indicates a two stage growth process of the oxide film. In the very beginning stage the substrate i.e., metallic lead undergoes normal electrochemical etching process and a uniform layer of oxide film is formed all over the substrate. However, in the second stage the application of pulse effectively induces a localized field gradient that results in variation of charge transfer at specified localized sites. Hence it favors the formation of vertically aligned nano walls structures. While in the case of normal potentiodynamic anodization process [12], the growth of oxide predominantly takes place by the growth of three dimensional clusters and subsequence coalescence. However, a detail study on the growth of the nano walls is in progress.

Photoelectrochemical studies:

The PEC response of the anodized lead electrode was studied in two different mediums using $Fe(CN)_6^{-4/-3}$ as an active electrolyte. The photocurrent variation at different applied potentials under chopped white light illumination condition is shown in Figure-7. The photocurrent attains the maxima at an applied bias of 1 V. An onset potential for anodic photocurrent is observed at -0.52 V with a blocking zone of ~1.5 V (-0.52 to 1 V). However, when the active electrolyte is used in ionic liquid medium the blocking zone extends to ~ 3.7 V (-0.67 to 3 V) with an onset potential for anodic photocurrent at -0.67 V.

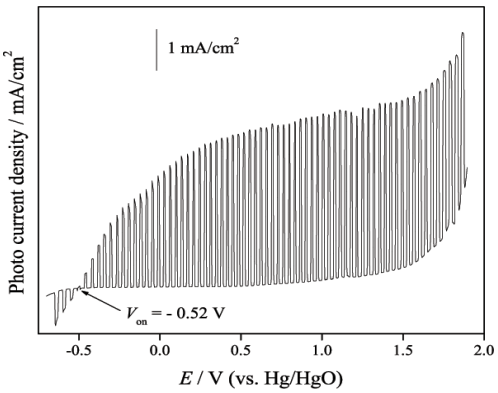

Fig: 7. The photocurrent response of the PbO_x electrode in aqueous active electrolyte of 0.1 M $K_4Fe(CN)_6$ /0.01 M $K_3Fe(CN)_6$ (pH 9.2) under chopped white light illumination condition at an incident light intensity of 100 mW/cm^2

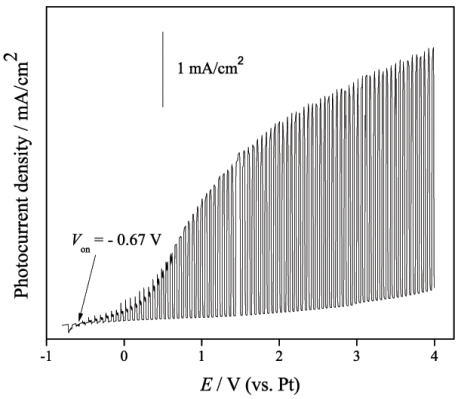

Fig: 8. The photocurrent response of the PbO_x electrode in active electrolyte of saturated $K_4Fe(CN)_6/K_3Fe(CN)_6$ in BMIm Cl^- ionic liquid under chopping white light illumination condition at an incident light intensity of 100 mW/cm^2

The parameters extracted from the photocurrent spectra are listed in Table.2. Comparison of Figures-7 and 8 clearly indicates that the nature of photo response is quite complicated in ionic liquid medium. While in aqueous medium the photocurrent enhances at a uniform rate from the flatband region to the photocurrent saturation region (Figure-7), the rate of enhancement of photocurrent in the case of ionic liquid medium is very sluggish at the initial stage from the flatband region (-0.67 to 1V) and then uniform towards the photocurrent saturation zone. This interesting observation clearly indicates that the ionic liquid is not a suitable medium for fabricating PEC device based on nonstoichiometric lead oxide.

Mott-Schottky studies:

In aqueous medium: Mott-Schottky plot shown in Figure-9 at different applied frequencies clearly indicates a flatband potential of -0.55 V, which is more negative than the onset potential (-0.52 V) of anodic photocurrent found in PEC studies. This can be explain by the Gartner Butler (GB) model [24,25] , which states that a diffusion of photogenerated minority carriers to the electrode surface in the absence of any electric field leading to a non-zero photocurrent at V_{fb} and hence V_{on} in PEC measurement will shift towards a positive potential for n-type semiconductor. In aqueous medium, two different slopes at higher frequencies clearly indicate the presence of two different doping levels in the oxide semiconductors. Dopping density values of 3.65×10^{15} and 1.67×10^{14} are corresponds to shallow and deep level states, respectively.

In ionic liquid medium: The Mott-Schottky study of the prepared electrode was also performed in the ionic liquid medium. We noticed from inset of Figure-10 that at higher frequencies (> 1 kHz) the contribution from the Helmholtz capacitance in addition to the space charge capacitance is prominent. Due to the variation in the Helmholtz capacitance of the ionic liquid/n-type electrode interface, it is very difficult to accurately determine the flat band potential by capacitance-voltage measurements. On the contrary, at lower frequencies we found a non-ideal Mott-Schottky characteristic**s**. This non ideality can be attributed to the electrode surface geometry, different level of donor states and the inhomogeneous adsorption of ionic species at the electrode surface. Formation of double layer is affected due to the arrangement of the large cations in the ionic liquid side [26]. As a result formation of more than one inner Helmholtz layer is expected at the semiconductor ionic liquid interface besides the usual double layer contributed by the active $Fe(CN)_6^{-4/-3}$ system. Due to this effect, three different level of donor sites are observed at lower frequencies. Also the non-ideal double layer formation due to existence of inter-wall pores influences the behavior.

Table: 2. Parameters obtained from the PEC studies

Electrolyte	J_{ph} mA/cm^2	V_{on} V	Potential Window V
Aqueous (9.2 pH)	4.03	-0.52	1.7
BMIm Cl^-	3.01	-0.67	3.7

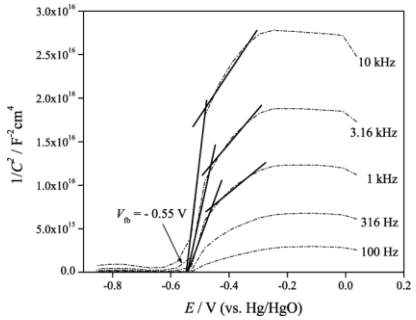

Fig: 9. Mott-Schottky plot for the oxide film in aqueous active electrolyte of 0.1 M $K_4Fe(CN)_6$ /0.01 M $K_3Fe(CN)_6$ (pH 9.2).

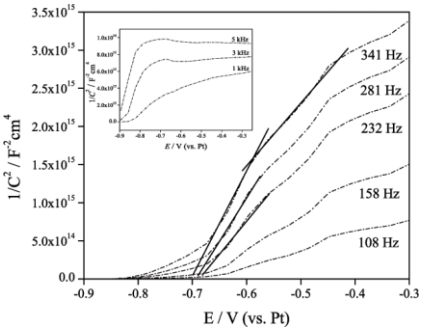

Fig: 10. Mott-Schottky plot at lower and higher (insect) frequencies for the oxide film in saturated $K_4Fe(CN)_6/K_3Fe(CN)_6$ in ionic liquid.

Energy conversion (JV) studies:

The power conversion efficiency curves for a PEC cell of anodized film with an active electrolyte in aqueous and ionic liquid mediums are shown in Figures-11 and 12, respectively. The open circuit voltage and a short circuit current were found to be 768 mV and 3.01 mA/cm^2 in aqueous medium. The maximum power conversion efficiency found was 0.87% with a fill factor of 0.37. Resistive nature of the lead oxide film is attributed to the high series resistance of the cell which lowers the fill factor and hence the power conversion efficiency. On the other hand JV response in ionic liquid showed open circuit voltage and short circuit current of 273 mV and 0.38 mA/cm^2 with the power conversion efficiency of 0.03%. Shifting of redox potential of an active electrolyte in ionic liquid results in lowering of the open circuit voltage while forming non-linear junction with the PbO_x. Very low conversion efficiency is attributed to the slow redox reaction rate of the active electrolyte in ionic liquid medium. This efficiently helps the recombination of the photogenerated carries in the semiconductor.

Stability Studies:

The photoanodic behaviour of anodized electrode under continuous illumination conditions was studied in both the mediums. The results for

aqueous and ionic liquid electrolytes are presented in Figure-13 and 14, respectively. It was observed that the short circuit current decreases continuously with illumination time for both the electrolytes. While the decrease in photocurrent in the aqueous medium is rather slow, the rate of decrease of photocurrent in ionic liquid medium is much faster for initial photocurrent decay process. The unwanted recombination of the photogenerated carriers facilitated by the slow redox reaction in the ionic liquid medium may be attributed to the observed phenomena.

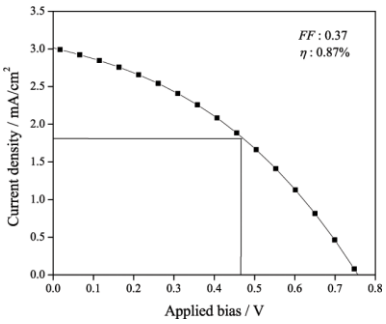

Fig: 11. The JV characteristic of the lead oxide electrode in 0.1 M $K_4Fe(CN)_6$ /0.01 M $K_3Fe(CN)_6$ in aqueous electrolyte (pH 9.2) upon white light illumination of 100 mW/cm^2 input light intensity.

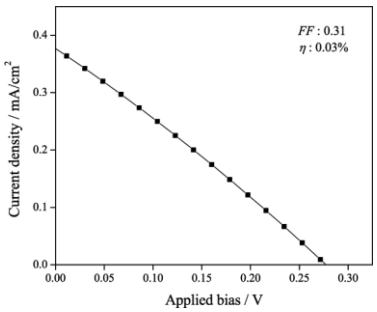

Fig: 12. The JV characteristic of the lead oxide electrode in saturated $K_4Fe(CN)_6$/ $K_3Fe(CN)_6$ in BMIm Cl^- ionic liquid upon white light illumination of 100 mW/cm^2 input light intensity.

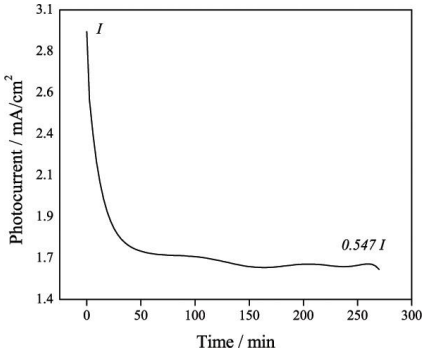

Fig: 13. Variation in short circuit photocurrent with time of illumination for anodized film in 0.1 M $K_4Fe(CN)_6$/0.01 M $K_3Fe(CN)_6$ in aqueous (pH 9.2)

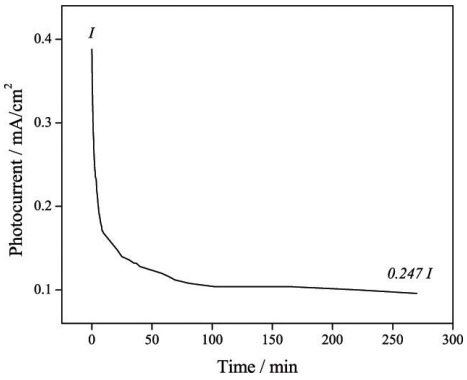

Fig: 14. Variation in short circuit photocurrent with time of illumination for anodized film in BMIMCl− ionic liquid

Conclusion:

In conclusion, the application of potential pulse lead to the formation of well-structured assembly of nano walls of lead oxide in a typical electrochemical synthesis process. The mechanism favors a localized growth process facilitate by the potential pulse after the initial process of anodization. The interconnected nano walls **enhance** the surface area of the electrode which ultimately enhances the absorption capability of active electrolyte. The PEC study indicates that ionic liquid is not a good medium for fabricating photoelectrochemical solar cell with PbO_x film due to very slow redox reaction kinetics. The photocurrent action spectra accordingly shows very low photocurrent of 0.38 mA/cm^2 in ionic liquid medium compared to 3.01 mA/cm^2 in aqueous medium. However, a very large extended blocking region of 3.7 V can be obtained by using ionic liquid medium. Study on detailed growth kinetics and impedance analysis of the oxide film in the ionic liquid medium is underway.

References:

1. J. S. Buchanan and L. M. Peter, Electrochim Acta, 1988, 33, 127–136.
2. R. G. Barradas, D. S. Nadezhdin, J. B. Webb, A. P. Roth and D. F. Williams, J Electroanal Chem, 1981, 126, 273–276.
3. M. Dimitrov, K. Kochev and D. Pavlov, J Electroanal Chem, 1985, 183,
4. R. G. Barradas and D. S. Nadezhdin, J Electroanal Chem, 1986, 202,
5. D. Pavlov, Electrochim Acta, 1978, 23, 845–854.
6. S. Fletcher and D. B. Matthews, J Electroanal Chem, 1981, 126, 131–144.
7. F. Caldara, A. Delmastro, G. Fracchia and M. Maja, J Electrochem Soc, 1980, 127, 1869–1876.
8. C. Pu, Z. L. He and W. F. Zhou, J Power Sources, 1992, 39, 233–237.
9. J. Han, Z. Pu and W. F. Zhou, J Electroanal Chem, 1994, 368, 43–46.
10. D. Pavlov, S. Zanova and G. Papazov, J Electrochem Soc, 1977, 124, 1522–1528.
11. V. I. Birss and M. T. Shevalier, J Electrochem Soc, 1987, 134, 802–808.

12. P. Veluchamy, M. Sharon, H. Minoura, Y. Ichinashi and K. Basavaswaran, J Electrochem Soc, 1993, 344, 73–89.
13. J. Burbank, J Electrochem Soc, 1959, 106, 369–376.
14. I. Mukhopadhyay, M. Raghavan, M. Sharon, H. Minoura and P. Veluchamy, J Electroanal Chem, 1994, 379, 531–534.
15. P. Veluchamy and H. Minoura, J Electrochem Soc, 1995, 142, 1799–1805.
16. P. Veluchamy, M. Sharon and D. Kumar, J Electroanal Chem, 1991, 315, 293–299.
17. P. Veluchamy, M. Sharon, M. Shimizu and H. Minoura, J Electroanal Chem, 1994, 371, 205–213.
18. I. Mukhopadhyay, S. Ghosh and M. Sharon, Surf Sci, 1997, 384, 234–239.
19. S.-J. Xia, PhD thesis, Fudan University, 1994.
20. J. C. Schootmiller, J Appl Phys, 1966, 37, 3505–3510.
21. P. D. F. Cards, 5-561, 4-686, 37-517, 23-353, 1987.
22. M. Sharon, I. Mukhopadhyay and S. Ghosh, J Solid State Electrochem, 1999, 3, 141–147.
23. G. Hodes, Gratzel M(ed) Energy resources through photochemistry and catalyst, Academic Press Technical Report Chapter 13, 1983.
24. W. W. Gartner, Phys Rev, 1959, 116, 84–87.
25. M. A. Butler, J Appl Phys, 1977, 48, 1914–1920.
26. M. Islam, M. Alam and T. Ohsaka, J Phys Chem, 2008, 112, 16568–16574.